Available online at www.sciencedirect.com
SCIENCE DIRECT®
International Journal of Mass Spectrometry 230 (2003) 45–55
International Journal of Mass Spectrometry
www.elsevier.com/locate/ijms

Fragmentation patterns of DNA–benzo(*a*)pyrene diol epoxide adducts characterized by nanoflow LC/quadrupole time-of-flight mass spectrometry

Jin J. Wang [a,*], William D. Marshall [b], Brandon Law [a], Daniel M. Lewis [a]

[a] *U.S. Department of Health and Human Services, Heath Effects Laboratory Division, Centers for Disease Control and Prevention, National Institute for Occupational Safety and Health, 1095 Willowdale Road, Morgantown, WV 26505, USA*
[b] *Department of Food Science & Agricultural Chemistry, McGill University, 21111 Lakeshore Road, Ste-Anne-de-Bellevue, Canada H9X 3V9*

Received 3 June 2003; accepted 13 August 2003

Abstract

Polycyclic aromatic hydrocarbons are a pervasive and abundant class of environmental and workplace pollutants. Formation of covalent DNA adducts has been considered to be a useful dosimeter or molecular biomarker for assessing the exposure to such pollutants. The establishment of prospective models for the formation of DNA adducts may help to understand the mechanisms of the effects. To identify the DNA adducts in this study, the fragmentation patterns of DNA–benzo(*a*)pyrene diol epoxide adducts were characterized by nanoflow liquid chromatography (LC) coupled to hybrid quadrupole orthogonal acceleration time-of-flight mass spectrometry (Q-TOF-MS). In the experiment, the DNA adducts were synthesized by reaction of calf thymus DNA with *anti*-benzo(*a*)pyrene-*r*-7,*t*-8-dihydrodiol-*t*-9,10-epoxide(±) (*anti*-BPDE). The major adducts of N^2-deoxyguanosine–benzo(*a*)pyrene-7,8-dihydrodiol-9,10-epoxide (N^2-dG–BPDE), N^6-deoxyadenosine–benzo(*a*)pyrene-7,8-dihydrodiol-9,10-epoxide (N^6-dA–BPDE), N^4-deoxycytidine–benzo(*a*)pyrene-7,8-epoxide (N^4-dC–BPDE), and N^3-deoxythymidine–benzo(*a*)pyrene-7,8-dihydrodiol-9,10-epoxide adduct (N^3-dT–BPDE) were identified by electrospray positive ionization with TOF-MS/MS scan mode. The results of this study demonstrated that the approach that utilizes collision-induced dissociation leading to a characteristic fragmentation pattern offers a distinct advantage for identification and elucidation of molecular structural features of the DNA adducts. The fragmentation patterns established in this study may be applied to identify DNA adducts in biological systems.

Keywords: DNA adducts; Nanoflow LC/Q-TOF-MS

1. Introduction

Polycyclic aromatic hydrocarbons (PAHs) are a class of toxicants that have been found in environment and workplaces [1–4]. Inhaled PAHs have long been suspected of inducing lung cancer [5,6]. It is generally believed that adduct formation by the interaction of a chemical or metabolized chemical with cellular DNA plays an essential role in the initial step of mutations and neoplastic cell transformations that can lead to chemical carcinogenesis. The adducts can thus serve as molecular biomarkers suitable for use in risk assessment [7–10]. Furthermore, the levels of DNA adducts can be used to document exposure to specific chemical hazards, to signal the onset of adverse health effects, and/or to identify individuals with susceptibility to certain threats particularly in workplaces. For these reasons, much effort has been directed toward the identification of DNA adducts. The development of a highly sensitive and reliable method for their identifications, however, pose considerable challenges due to the complexities associated with the adduct molecular structures and chemical characteristics.

Several different methods such as immunoassay, radiopostlabeling, and high-performance liquid chromatography (HPLC) with ultraviolet or fluorescence detection have been used to assay DNA adducts [11]. Postlabeling with ^{32}P is the most widely accepted method. This method involves the enzymatic transfer of radiolabeled phosphate groups from [^{32}P] ATP to nucleotides, separation of carcinogen-modified nucleotides from normal nucleotides, and quantification based on radioactivity. The detection limit of this approach can be as low as one adduct per 10^9 normal nu-

* Corresponding author. Tel.: +1-304-285-6329; fax: +1-304-285-6126.
E-mail address: juw9@cdc.gov (J.J. Wang).

1387-3806/$ – see front matter © 2003 Published by Elsevier B.V.
doi:10.1016/j.ijms.2003.08.004

cleotides [12]. A major deficiency of these methods is that they cannot provide specific information on the chemical identity of the adduct(s) or the toxic progenitor(s), which is essential to obtain a comprehensive understanding of the contributions of the adducts to carcinogenesis. Some of the methods also lack sensitivity inherent in certain procedures of the identification and measurement.

The direct analysis of DNA adducts using LC combined with mass spectrometry is increasing [13–16]. With selected ion monitoring, the sensitivity of detection can be enhanced from 10- to 100-fold. When capillary LC or electrophoresis is used in conjunction with MS/MS, it is possible not only to detect target adducts, but also to generate a wealth of structural information. The application of the LC/MS system can also obviate those problems arising from the use of chemical derivatization that is required for gas chromatography–mass spectrometry (GC–MS) analysis. Model adducts of benzo(*a*)pyrene and nucleosides have been studied [17], in which a HPLC and fast atom bombardment (FAB) MS/MS were used. Identifications of the major adducts formed by reaction of benzo(*a*)pyrene diol epoxide (BPDE) with DNA in vitro were reported with GC–MS method [18]. Detection of deoxyguanosine–BPDE utilizing capillary electophoresis coupled with negative ionization MS has also been reported [19]. However, the method for the characterization of the DNA–PAH adducts using advanced MS techniques have not been well established.

In our previous study, benzo(*a*)pyrene was found in asphalt fume [20], and its diol expoxide metabolite was identified in the urine of asphalt fume exposed mice [21]. The overall goal of this study was to develop a sensitive method to analyze the DNA adducts needed to investigate the mechanisms of adverse health effects associated with occupational exposure to asphalt fume. To achieve this goal, the specific aims of the current study were: (i) to develop a set of practical experimental procedures to utilize a nanoflow LC/Q-TOF-MS technology for identifying the DNA adducts, (ii) to explore the capability of this instrumental approach in such application, and (iii) to characterize the fragmentation patterns of DNA–benzo(*a*)pyrene diol epoxide adducts.

2. Materials and methods

2.1. Chemicals and instrumentation

Reagent grade dichloromethane (CH_2Cl_2, 99.9%), hexane (capillary GC grade), methanol, acetonitrile, and formic acid were purchased from Aldrich (Milwaukee, WI, USA). Benzo(*a*)pyrene-7,8-dihydrol-9,10-epoxide(±) was purchased from NCI Chemical Carcinogen Reference Standard Repository (Kansas, MI, USA). Calf thymus DNA and [Glu]-fibrinopeptide B were obtained from Sigma Chemical Co. (St. Louis, MO, USA).

Solid phase extraction cartridges of C_{18} (500 mg/2.8 ml) was purchased from Varian (Harbor City, CA, USA). PTFE tubes (30 ml) and glass tubes (10 ml) were purchased from Fisher Scientific (Pittsburgh, PA, USA). Target DP vials (1.5 mm with 200 μl inserts) were obtained from Alltech Associates, Inc. (Deerfield, IL, USA). Syringe filter (25 mm, 0.2 μm pore size; Gelman Sciences, Ann Arbor, MI, USA) was employed to perform the purification and filtration of the sample solutions. Samples were concentrated under a nitrogen stream using a TurboVap® LV evaporator (Zymark). Liquid nitrogen, high purity helium, and argon were purchased from Butler Gas Products Co. (Mckees Rocks, PA, USA), and used as carrier gases for Q-TOF-MS II (Micromass Inc., Beverly, MA, USA). The nanoflow LC column was a NAN75-15-03-C_{18} (75 μm i.d., 3 μm, 100 Å; LC Packings, San Francisco, CA, USA).

2.2. Synthesis DNA adducts

Test adducts of DNA–benzo(*a*)pyrene-7,8-dihydrodiol-9,10-epoxide were synthesized by reaction of calf thymus DNA with *anti*-benzo(*a*)pyrene-7,8-diol-9,10-epoxide (*anti*-BPDE) as described by Barry et al. [19]. Briefly, approximately 15 mg of calf thymus DNA was dissolved in 10 ml of 0.05 M Tris–HCl solution (pH 6.8), and 2 mg of *trans*-benzo(*a*)pyrene-7,8-diol-9,10-epoxide was dissolved in 2 ml of methanol. Then the second solution was added to the calf thymus DNA solution. The resultant mixture was incubated at 50 °C for ∼48 h. Unreacted BPDE in the solution was extracted with ethyl acetate (6 ml) and diethyl ether (2 ml). The DNA was precipitated with NaCl (0.2 M) in cold ethanol (10 ml). The sample solution was then centrifuged at −10 °C for 30 min at 12,000 rpm. The DNA pellet was collected and stored at −20 °C until enzymatic digestion.

2.3. DNA adducts purification

To release the dioxynucleoside, the synthesized DNA adducts were digested enzymatically with DNase I, nuclease P1, and phosphodiesterase [20]. Briefly, DNA sample (2 mg) was dissolved in 2 ml 5 mM Tris–HCl and 10 mM $MgCl_2$ (pH 7.4). DNase I (10 mg/ml in 0.9% saline) was added at 200 μg of enzyme/ml and incubated for 1 h at 37 °C. Then 20 μl of nuclease P1 (1 mg/ml in 1 mM $ZnCl_2$) was added and incubated for a further 6 h at 37 °C. Alkaline phosphatase was added at 2 units/ml, and the incubation was continued for 24 h at 37 °C. The enzyme-digests were then subjected to a solid phase extraction. The C_{18} cartridge was pre-conditioned with H_2O followed by 60% H_2O + 40% ACN, loaded with crude digest then washed with H_2O. The DNA adducts were eluted from the cartridge with 50% (v/v) ACN:H_2O. After filtration, the sample was concentrated under a gentle stream of nitrogen.

2.4. Nanoflow LC/Q-TOF-MS

The nanoflow (140 nl/min) LC was coupled to a hybrid Q-TOF-MS. The operational features of the Q-TOF-MS sys-

tem consisted of a standard Z-spray source fitted with a heated nebulizer probe. The electrospray ionization combined with TOF-MS/MS was used for selected precursor ion detection. The collision energy was optimized to generate characteristic fragmentation patterns. The source temperature was maintained at 90 °C. The instrument was calibrated with a multi-point calibration technique using selected fragment ions (*m/z*: 333, 480, 684, 813, 942, 1056, and 1285) that resulted from the collision-induced decomposition of [Glu]-fibrinopeptide B (Sigma Chemical Co.). A gradient elution profile was generated with 0.1% acetic acid in acetonitrile (Solvent A) and 0.1% acetic acid in methanol (Solvent B). A NAN75-15-03-C_{18} column (75 μm i.d., 3 μm, 100 Å) was used to separate target analyte from interferences. Under the optimized condition, the signal to noise ratio from a consumption of 20 fmol of [Glu]-fibrinopeptide B was greater than 3:1 for the most intense fragment ions of TOF-MS/MS acquisition. The linear dynamic range was approximately 3 orders of magnitude (0.05–40 pmol). In all cases, calibration regression coefficients were between 0.95 and 0.99. The precision was determined with five replicate injection (R.S.D. = ±18%). Once optimized, operating parameters were maintained constant for the duration of the experiments.

3. Results

3.1. Fragmentation pattern of N^2-deoxyguanosine–benzo(a)pyrene diol epoxide adduct

The protonated precursor ion *m/z* 570 ($C_{30}H_{27}O_7N_5$ + H)$^+$ was selected to monitor adduct of N^2-deoxyguanosine–benzo(*a*)pyrene-7,8-dihydrodiol-9,10-epoxide. A characteristic tandem MS fragmentation pattern was acquired by setting a precursor-ion produced at 1 amu detection window under scanning the first quadrupole, and a product-ion spectrum produced by maintaining the first quadrupole at constant *m/z* while scanning the TOF-MS/MS. Adduct elution (140 nl/min) from the capillary column was conducted with 0.1% acetic acid in acetonitrile–methanol (1:1 v/v). The resolution of TOF-MS/MS acquisition was adjusted to ~8000. The detection limits ranged from 30 to 50 pg based on the signal to noise ratio greater than 3:1 for purified DNA adducts. The TOF-MS/MS scan mode with selected precursor ion *m/z* 570 was edited to monitor N^2-dG–BPDE adduct. Following the optimization of the system conditions, the N^2-dG–BPDE adduct was eluted from the nanoflow C_{18} column after 3.73 min (Fig. 1a). With selected single precursor ion monitoring, separation

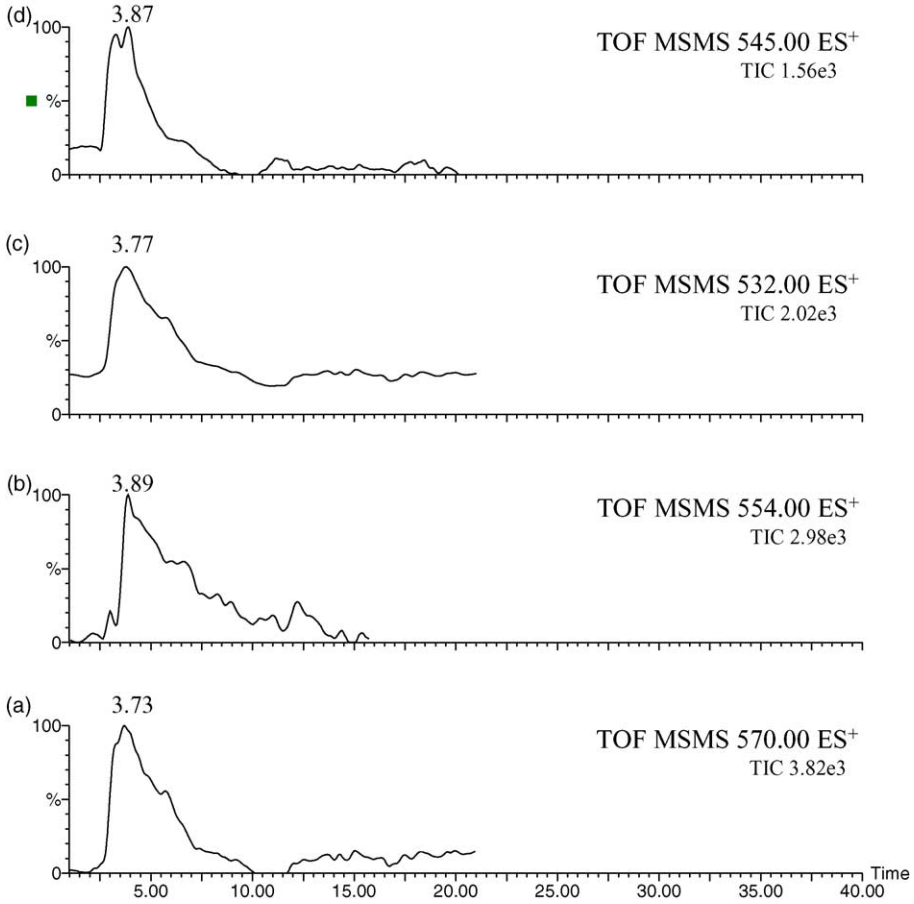

Fig. 1. TOF-MS/MS scans with selected precursor ions: (a) dG–BPDE adduct (MH^+, 570), (b) dA–BPDE adduct (MH^+, 554), (c) dC–BPDE adduct (MH^+, 532), and (d) dT–BPDE adduct (MH^+, 545).

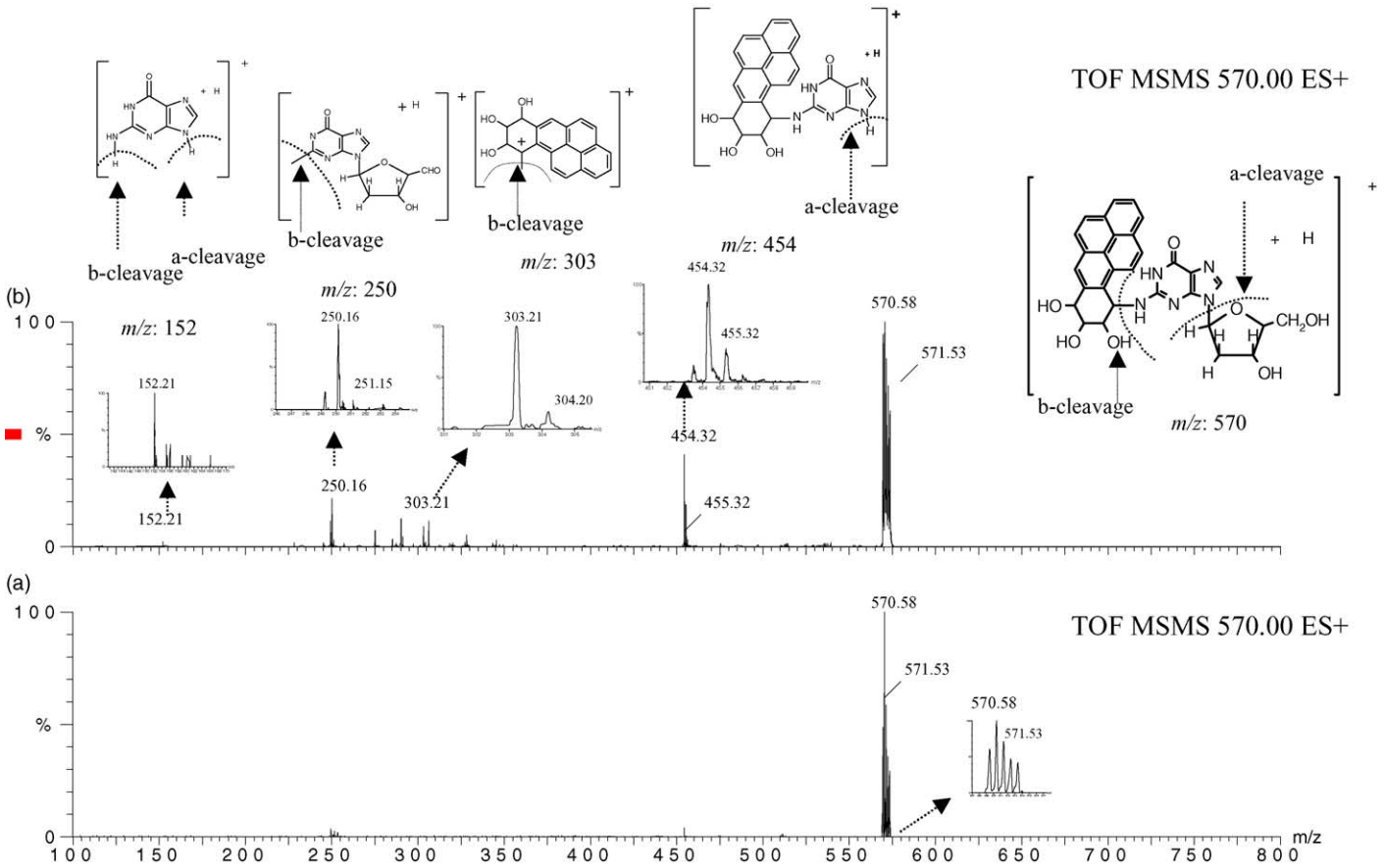

Fig. 2. A characteristic fragmentation pattern of N^2-deoxyguanosine–benzo(*a*)pyrene-7,8-dihydrodiol-9,10-epoxide adduct acquired at (a) low collision energy (8 eV), and (b) high collision energy (15 eV).

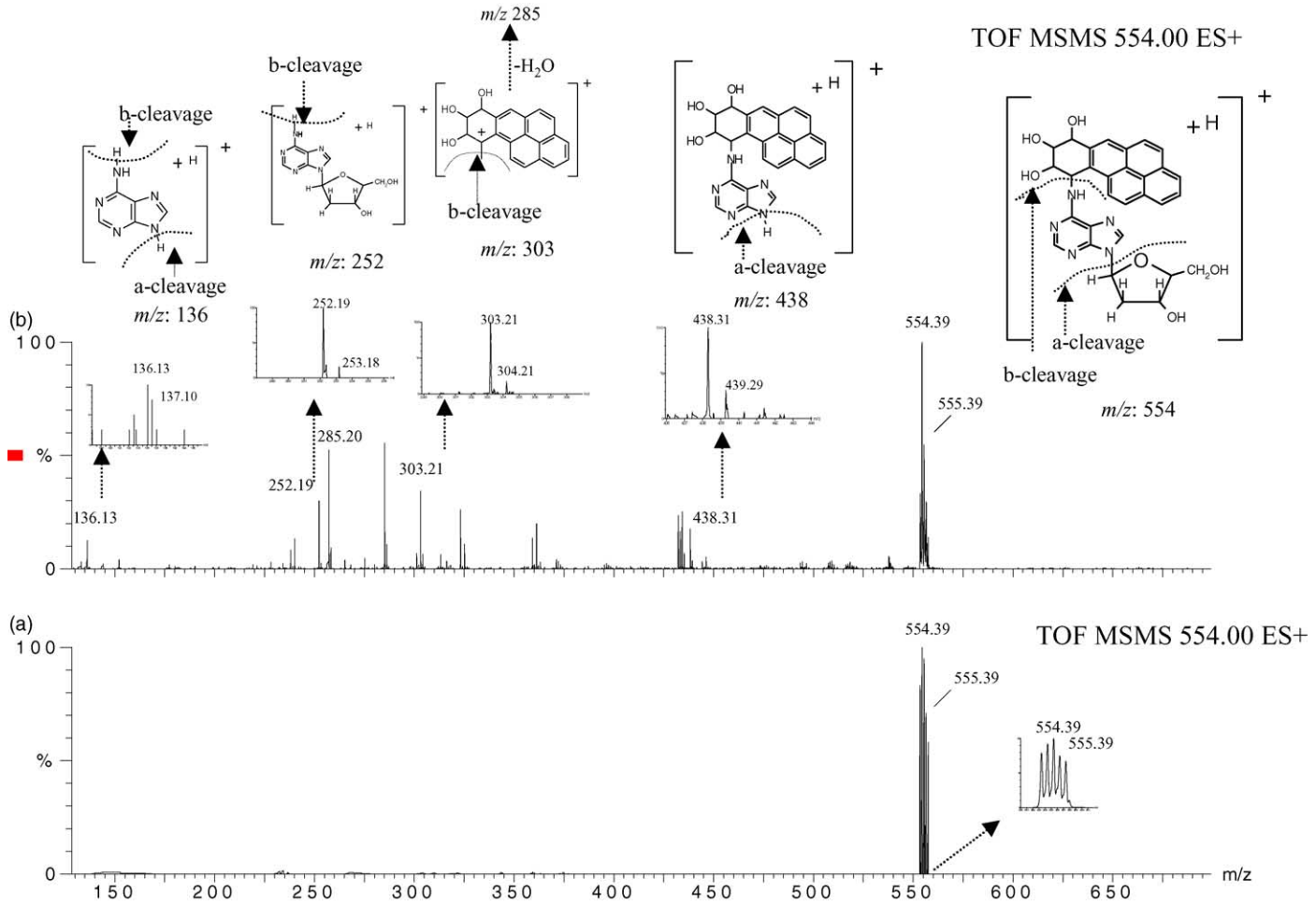

Fig. 3. A characteristic fragmentation pattern of N^6-deoxyadenosine–benzo(*a*)pyrene-7,8-dihydrodiol-9,10-epoxide adduct acquired at (a) low collision energy (8 eV), and (b) high collision energy (25 eV).

of analytes by nanoflow column was not the major consideration.

The column was used to introduce sample into the MS and to improve the sensitivity by increasing the back pressure. A fragmentation pattern characteristic of the N^2-dG–BPDE adduct is presented in Fig. 2. To increase the selectivity of an assay for a given adduct, the collision energy was varied for each specific run. A TOF-MS/MS spectrum with the low collision energy (8 eV) is presented in Fig. 2a. A singly-charged N^2-dG–BPDE adduct molecular ion (*m/z* 570.58) was the only major ion to be observed with this experimental condition. However, when the collision energy was increased to 15 eV, appreciable fragmentation was observed (Fig. 2b). Meanwhile, it was noticed that when the collision energy was increased, the total ion counts increased, but the precursor ion counts decreased. A strong singly-charged adduct of N^2-dG–BPDE was observed at *m/z* 570.58 $(C_{30}H_{27}O_7N_5 + H)^+$ with M + 1 peak (*m/z* 571.53). A proposed fragmentation pathway for this molecular ion is summarized in Fig. 2. Two main cleavages (a- and b-) were predicted to occur. Four major fragment ions with M+1 peak were observed in the MS/MS spectrum. The spectrum indicated that the fragment *m/z* 454.32 [$(C_{25}H_{19}O_4N_5 + H)^+$, M + 1 peak, *m/z* 455.3217] corresponded to a-cleavage and it was the primary fragment at this experimental setting. The fragment *m/z* 303.21 $(C_{20}H_{14}O_3 + H)^+$ corresponded to b-cleavage. The fragment *m/z* 250.16 $(C_{10}H_9O_4N_4 + H)^+$ had lost –NH from guanine and $–H_2$ from the sugar moiety corresponded to b-cleavage. The fourth fragment at *m/z* 152.21 $(C_5H_5ON_5 + H)^+$, corresponded to both a- and b-cleavages. The results indicated that the characteristic tandem MS/MS fragmentation pattern of the molecular ion presented distinct features for DNA adduct identification.

3.2. Fragmentation pattern of N^6-deoxyadenosine–benzo (*a*)pyrene diol epoxide adduct

The protonated precursor ion *m/z* 554 $(C_{30}H_{27}O_6N_5+H)^+$ was selected to monitor adduct of N^6-deoxyadenosine–benzo(*a*)pyrene-7,8-dihydrodiol-9,10-epoxide. A TOF-MS/MS scan mode was edited to monitor N^6-dA–BPDE adduct. Following the optimization of the system conditions, the N^6-dA–BPDE adduct was eluted from the nanoflow C_{18} column after 3.89 min (Fig. 1b). A characteristic fragmentation pattern of N^6-dA–BPDE adduct is summarized in Fig. 3. Under low collision energy (8 eV), a TOF-MS/MS spectrum is recorded in Fig. 3a. A strong singly-charged N^6-dA–BPDE adduct (*m/z* 554.39) was the only major ion to be observed at this condition. When the collision energy was increased to 25 eV, appreciable fragmentation was observed (presented in Fig. 3b). The singly-charged N^6-dA–BPDE adduct was observed at *m/z* 554.39 $(C_{30}H_{27}O_6N_5 + H)^+$ with M + 1 peak, *m/z* 555.39. Proposed fragmentation schemes have been included in Fig. 3. Two principle cleavages were anticipated corresponding to a- and b-cleavages. Five major fragment ions were observed. Whereas the fragment at *m/z* 438.31 [$(C_{25}H_{19}O_3N_5 + H)^+$, M + 1 peak, *m/z* 439.29] corresponded to a-cleavage, the fragment *m/z* 303.21 $(C_{20}H_{14}O_3 + H)^+$ corresponded to b-cleavage. Collision-induced dissociations can also cause dehydration to occur; the fragment at *m/z* 303.21 $(C_{20}H_{14}O_3 + H)^+$ had lost one H_2O to form fragment *m/z* 285.20. The fragment *m/z* 252.19 $(C_{10}H_{13}O_3N_5 + H)^+$ corresponded to b-cleavage. The fourth fragment *m/z* 136.13 [$(C_5H_5N_5 + H)^+$, M + 1 peak, *m/z* 137.10] corresponded to the sum of both a- and b-cleavages.

3.3. Fragmentation pattern of N^4-deoxycytidine–benzo (*a*)pyrene diol epoxide adduct

The protonated precursor ion *m/z* 532 $(C_{29}H_{29}O_7N_3+H)^+$ was selected to monitor the adduct N^4-deoxycytidine–benzo (*a*)pyrene-7,8-dihydrodiol-9,10-epoxide. Following optimization of the system conditions, the N^4-dC–BPDE adduct was eluted from the nanoflow C_{18} column after 3.77 min (Fig. 1c). A characteristic fragmentation pattern of N^4-dC–BPDE adduct is presented in Fig. 4. The TOF-MS/MS spectrum at low collision energy (8 eV) is recorded in Fig. 4a. The intense singly-charged N^4-dC–BPDE adduct (*m/z* 532.33) was the only major ion to be observed at this condition. When the collision energy was increased to 20 eV, appreciable fragmentation was induced as presented in Fig. 4b. The singly-charged N^4-dC–BPDE adduct was observed at *m/z* 532.33 $(C_{29}H_{29}N_3O_7 + H)^+$. A proposed fragmentation pathway is summarized in Fig. 4. Two main cleavages (a- and b-) were predicted to occur. Three major fragments were observed in TOF-MS/MS spectrum. Whereas the fragment, *m/z* 416.28 $(C_{24}H_{21}N_3O_4 + H)^+$, corresponded to a-cleavage, the fragment at *m/z* 303.20 $(C_{20}H_{14}O_3 + H)^+$ corresponded to b-cleavage, that lost a further three H_2O to form fragment *m/z* 249.20. The fragment *m/z* 230.28 $(C_9H_{15}N_3O_4 + H)^+$ was the other fragment that resulted from b-cleavage.

3.4. Fragmentation pattern of N^3-deoxythymidine–benzo (*a*)pyrene diol epoxide adduct

The protonated precursor ion *m/z* 545 $(C_{30}H_{28}O_8N_2+H)^+$ was selected to monitor adduct of N^3-deoxythymidine–benzo (*a*)pyrene-7,8-dihydrodiol-9,10-epoxide. A TOF-MS/MS scan mode was edited to monitor N^3-dT–BPDE adduct. Following the optimization of the system conditions, the N^3-dT–BPDE adduct was eluted from the nanoflow C_{18} column after 3.87 min (Fig. 1d). A characteristic fragmentation pattern of N^3-dT–BPDE adduct was presented in Fig. 5. The TOF-MS/MS spectrum that resulted from low collision energy (8 eV) is presented in Fig. 5a. A strong singly-charged N^3-dT–BPDE adduct ion (*m/z* 545.35) was the only major ion to be observed at this condition. When the collision energy was increased to 15 eV, appreciable fragmentation was observed (Fig. 5b). A singly-charged N^3-dT–BPDE adduct

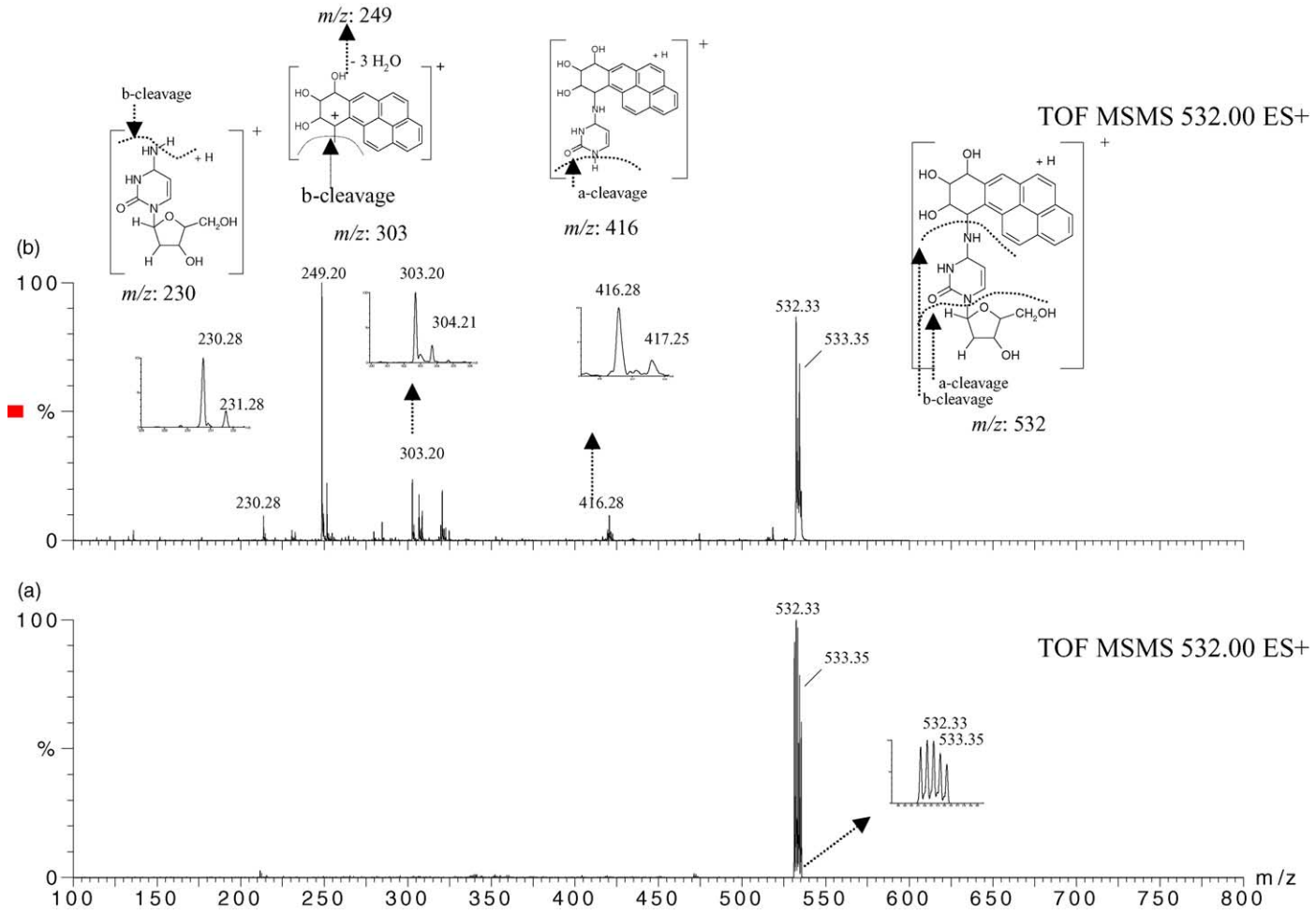

Fig. 4. A characteristic fragmentation pattern of N^4-deoxycytidine–benzo(*a*)pyrene-7,8-dihydrodiol-9,10-epoxide adduct acquired at (a) low collision energy (8 eV), and (b) high collision energy (20 eV).

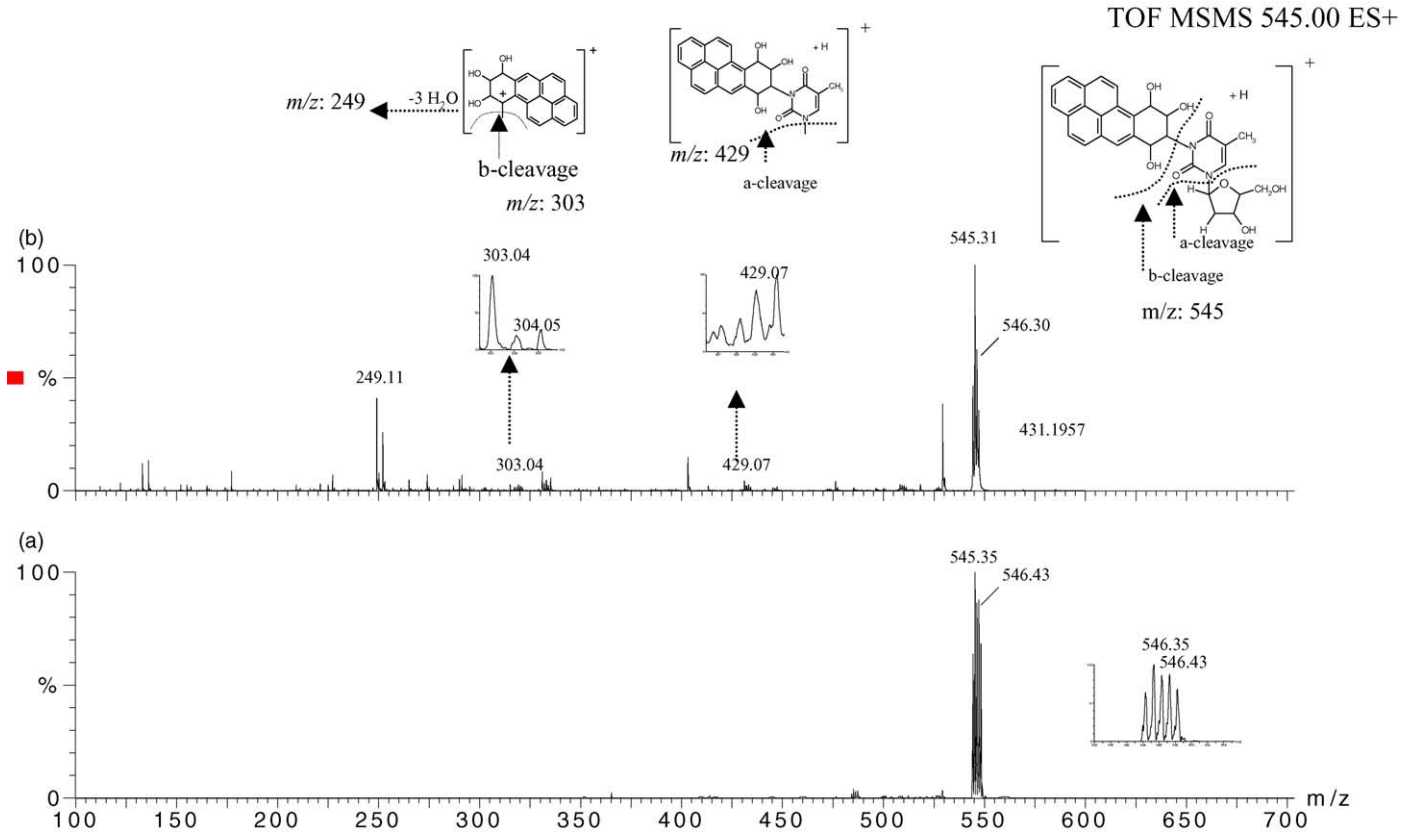

Fig. 5. A characteristic fragmentation pattern of N^3-deoxythymidine–benzo(*a*)pyrene-7,8-dihydrodiol-9,10-epoxide adduct acquired at (a) low collision energy (8 eV), and (b) high collision energy (15 eV).

was observed at *m/z* 545.31 $(C_{30}H_{28}N_2O_8 + H)^+$. A proposed fragmentation pathway is illustrated in Fig. 5. Two main cleavages were predicted to occur corresponding to a- and b-cleavages. Three major fragments were observed in the TOF-MS/MS spectrum. The fragment *m/z* 429.07 corresponded to a-cleavage. The fragment *m/z* 303.04 $(C_{20}H_{14}O_3 + H)^+$ corresponded to b-cleavage, and when it lost three H_2O, fragment *m/z* 249.11 was formed.

Table 1
Potential of benzo(*a*)pyrene diol epoxide adducts formation in DNA

BPDE–DNA	Adduct structure	BPDE–DNA	Adduct structure
BPDE–N^1-dG	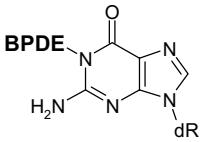	BPDE–N^1-dA	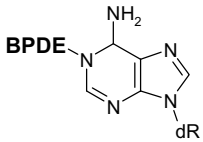
BPDE–N^2-dG	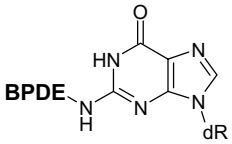	BPDE–N^3-dA	
BPDE–N^3-dG	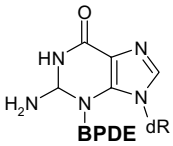	BPDE–N^6-dA	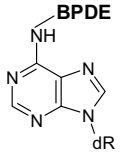
BPDE–O^6-dG	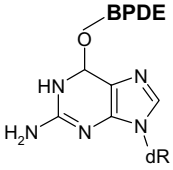	BPDE–N^7-dA	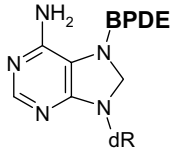
BPDE–N^7-dG	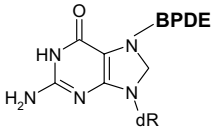		
BPDE–O^2-dC	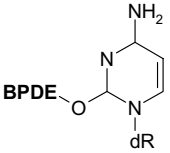	BPDE–O^2-dT	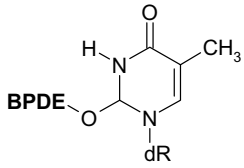
BPDE–N^3-dC	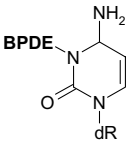	BPDE–N^3-dT	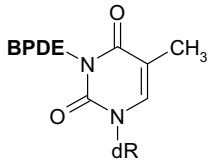
BPDE–N^4-dC	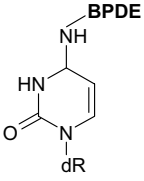	BPDE–O^4-dT	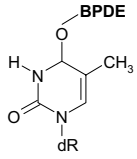

BPDE: 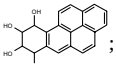 ; dR: 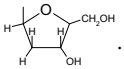 .

4. Discussion

In the current study, a set of experimental procedures was developed to characterize DNA adducts based on a nanoflow LC/Q-TOF-MS technique. With the experimental conditions as described, the greatest ion intensities were observed under proton transfer conditions.

Although the retention times for DNA adducts from the capillary column without performing gradient elution were poorly resolved (Fig. 1), it was still possible to characterize the target adducts of dG–BPDE, dA–BPDE, dC–BPDE, and dT–BPDE with specifically selected precursor ion within the TOF-MS/MS scan. This is a unique advantage of the current instrumental approach. Specifically, it was possible to deconvolute the complex mixture. The resolving power of nanoflow LC coupled with the sensitivity of hybrid Q-TOF-MS with electrospray ionization permits detection of fmol quantities of DNA adducts. This makes it possible to quantify DNA adducts in biological models. Compared with immunoassays and radio-postlabeling methods, the method developed in this study provides appreciable supplemental information.

The use of DNA adducts as molecular biomarker has generated considerable interest in study of mechanisms associated with the onset of several diseases as well as assessments of risks associated with occupational exposure to chemical toxicants. It has been generally accepted that covalent binding of chemicals to DNA resulting in DNA adducts is a common characteristic of many carcinogens and genotoxicants. The formation of certain types of DNA adducts is a crucial step in the induction of cancer and a primary stage in mutagenesis. Based on the adduct formation principle [22], 15 potential BPDE adducts can be formed with the four nucleic acid bases and they are postulated in our study. These include five adducts of dG–BPDE with two chemical formulae ($C_{30}H_{27}N_5O_7$, $C_{30}H_{29}N_5O_7$); four dA–BPDE adducts with two chemical formulae ($C_{30}H_{27}N_5O_6$, $C_{30}H_{29}N_5O_6$); three dC–BPDE adducts with two chemical formulae ($C_{29}H_{29}N_3O_7$, $C_{29}H_{31}N_3O_7$); and three dT–BPDE adducts with two chemical formulae ($C_{30}H_{28}N_2O_8$, $C_{30}H_{30}N_2O_8$) (Table 1). The tendency of the addition reactions to proceed at the various sites was anticipated to depend on the identity of the reactive species, the nucleophilicity of the reactive sites and steric factors. The nucleophilicity of the nitrogen (N^2) in deoxyguanosine was anticipated to create an active center that can serve as a nucleophile to form N^2-deoxyguanosine–BPDE adduct [23]. The structurally similar, N^6-deoxyadenosine site was anticipated to form a second dominant adduct with BPDE. Thus, N^2-dG–BPDE, N^6-dA–BPDE, N^4-dC–BPDE, and N^3-dT–BPDE were anticipated to be the primary adducts and were characterized in this study, although other adducts might also exist. However, the various isoforms of the DNA adducts were not investigated in this study because of the limitation of the technique.

Monitoring a metastable decomposition reaction by MS/MS provides a means of increasing the selectivity of an assay for a given analyte. The singly-charged precursor ion at *m/z* 570 (Fig. 2) was selected to characterize N^2-dG–BPDE. To further enhance the specificity of the assay for a given adduct, the collision energy was varied for each specific run. In comparison spectra acquired with low (8 eV) and high (15 eV) collision energy, it was observed that the singly-charged adduct was the only major ion at low collision energy (Fig. 2a). When the collision energy was increased to 15 eV (Fig. 2b), four prominent fragments were observed that corresponded to the anticipated cleavages. The results indicated that variations in the collision-induced dissociation energies present advantages for the identification of selected adducts. The similar fragmentation pathways were observed for N^6-dA–BPDE (Fig. 3). The results indicate that both N^2-dG–BPDE and N^6-dA–BPDE are stable adducts. By interpretation of the spectra of N^4-dC–BPDE (Fig. 4) and N^3-dT–BPDE (Fig. 5), the fragments of a-cleavage from both adducts were observed at low abundance. This suggested that there might be certain differences such as electrophilicity and steric constraints among these two adducts. Other factors contributing to low abundance fragments may include the relative instability of the various DNA adducts. The observed differences, however, do not change the fundamental characteristic fragmentation patterns. The major fragments from the collision-induced dissociation matched the postulated cleavages of the corresponding DNA adduct. Overall, the results obtained from the study provide a wealth of information to probe the molecular structures of these DNA adducts. To our knowledge, the DNA adducts formed with four kinds of nucleic acid and characterized with their specific fragmentation patterns by nanoflow LC/Q-TOF-MS has not been reported previously.

5. Summary

A mass spectrometric method was developed to characterize DNA adducts in biological matrices. The specific fragmentation patterns of benzo(*a*)pyrene-7,8-dihydrodiol-9,10-epoxide–N^2-deoxyguanosine, –N^6-deoxyadenosine, –N^4-deoxycytidine, and –N^3-deoxythymidine were quantified based on nanoflow LC coupled to Q-TOF-MS. The results of this study demonstrated that the method is sensitive. The approach, utilizing a collision-induced dissociation leading to a characteristic fragmentation pattern, provides increased selectivity for the identification of DNA adducts. A distinct advantage of the method is that it permits unambiguous chemical identification of DNA adducts and molecular structure information. The characteristic fragmentation patterns established in this study can be applied to identify DNA adducts in biological systems.

Acknowledgements

The authors gratefully thank Al Munson, Paul Siegel, Nancy Bollinger, Beverly Carter, and Judy Mull for their project support and coordination.

References

[1] M.L. Machado, P.W. Beatty, J.C. Fetzer, A.H. Glickman, E.L. McGinnis, Fundam. Appl. Toxicol. 22 (2) (1994) 317.
[2] A. Sivak, R. Niemeier, D. Lynch, K. Beltis, S. Simon, R. Salomon, R. Latta, B. Belinky, K. Menzies, A. Lunsford, C. Cooper, A. Ross, R. Bruner, Cancer Lett. 117 (1) (1997) 113.
[3] M.A. Butler, G. Burr, D. Dankovic, A. Lunsford, A. Miller, M. Nguyen, L. Olsen, D. Sharpnack, J. Snawder, L. Stayner, M.H. Sweeney, A. Teass, J. Wess, R. Zumwalde, A report of CDC/NIOSH, Health effects of occupational exposure to asphalt, 2000.
[4] C.C. Lutes, R.J. Thomas, R. Burnette, Evaluation of emissions from paving asphalts. Final Report to U.S. EPA, Prepared by Acurex Environmental Corporation, Research Triangle Park, NC, 1994.
[5] S. Kimberly, A brief review of “Health Effects Related to Occupational Exposure.” Howard University Hospital, Department of Emergency Medicine, 2001.
[6] I. Burstyn, H. Kromhout, T. Kauppinen, P. Heikkila, P. Boffetta, Ann. Occup. Hyg. 1 (2000) 43.
[7] M.C. Poirier, F.A. Beland, Chem. Res. Toxicol. 5 (1992) 749.
[8] J.A. Ross, G.B. Nelson, J.R. Rabinowits, G.D. Stoner, S. Nesnow, M. Mass, Polycycl. Arom. Comp. 10 (1996) 267.
[9] D. Rindgen, R.J. Turesky, P. Vouros, Chem. Res. Toxicol. 8 (1995) 1005.
[10] J. Wang, P.D. Siegel, D.M. Lewis, K. Ashley, L.E. Stettler, W.E. Wallace, E. Vo, Spectroscopic Techniques in Industrial Hygiene. Article A1321 in Encyclopedia of Analytical Chemistry, vol. 6, Wiley, New York, 2000.
[11] D.K. La, J.A. Swenberg, Mutat. Res. 365 (1996) 129.
[12] K. Randerath, E. Randerath, Drug Metab. Rev. 26 (1994) 67.
[13] H. Huan, J. Ahmedin, D. Connie, A. Steven, S.A. Barker, D.H. Swenson, J.C. Means, Anal. Biochem. 265 (1998) 139.
[14] L. Leclercq, C. Laurent, E.D. Pauw, Anal. Chem. 69 (1997) 1952.
[15] T.Y. Yen, N.I. Christova-Gueoguieva, N. Scheller, S. Holt, J.A. Swenberg, M.J. Charles, J. Mass Spectrom. 31 (1996) 1271.
[16] K. Vanhoutte, W.V. Dongen, H.I. Lemiere, E.L. Esmans, H.V. Onckelen, V. Eeckhout, R.E. Soest, A.J. Hudson, Anal. Chem. 69 (1997) 3161.
[17] N.V.S. RamaKrishna, F. Gao, N.S. Padmavathi, E.L. Cavalieri, E.G. Rogan, R.L. Cerny, M.L. Gross, Chem. Res. Toxicol. 5 (1992) 293.
[18] K.M. Straub, T. Meehan, A.L. Burlingame, M. Calvin, Proc. Natl. Acad. Sci. U.S.A. 74 (12) (1997) 5285.
[19] J.P. Barry, C. Norwood, P. Vouros, Anal. Chem. 68 (1996) 1432.
[20] J. Wang, D.M. Lewis, V. Castranova, D.G. Frazer, T. Goldsmith, S. Tomblyn, J. Simpson, S. Stone, A. Afshari, P.D. Siegel, Anal. Chem. 73 (15) (2001) 3691.
[21] J. Wang, D.G. Frazer, B. Law, D.M. Lewis, The Analyst 128 (2003) 864.
[22] Y. Zou, C. Luo, N.E. Geacintov, Biochemistry 40 (2001) 2923.
[23] D.K. La, J.A. Swenberg, Mutat. Res. 365 (1996) 129.